Computing Lie Algebras via the UNS: A Zero-Residue Approach

Garret Sobczyk* Jesus Cruz Guzman Bill Page

August 14, 2026

Abstract

The classification of complex simple Lie algebras and Clifford geometric algebras has historically relied on rigid metric signatures and top-down complexification. In this paper, we construct a strict bottom-up geometric origin for these symmetries. By defining a Universal Null Substrate (UNS) based on a Quadratic Space of Null Vectors (QSNV), we demonstrate that geometric algebras and Lie automorphisms emerge natively from orthogonal null simplexes. We introduce the algebraic "Valley of Stability," showing that geometric algebras crystallize into discretely defined structures via Zero-Residue Factorization, seamlessly reducing high-dimensional geometric multiplications to simple index arithmetic on the null substrate. When geometric strain forces degeneracy, the substrate sheds a nilpotent factor at a geometric singularity we term the Resonant Hub. Finally, we demonstrate that this Hub naturally stabilizes as the Anti-de Sitter algebra $\mathbb{G}_{2,3}$, providing a continuous, non-degenerate bridge to the conformal spacetime symmetries of $O(2,4)$ via Coxeter simplices.

1 The Constitution: Quadratic Space of Null Vectors

Standard Clifford geometric algebras $\mathbb{G}_{p,q}$ are traditionally defined by an orthonormal basis squaring to ± 1 [4, 6, 8]. We take a "Substrate-First" approach, defining the algebra via compatible null vectors [10, 7].

Definition 1 (**The Null Primitive**)**.** The fundamental element of the substrate is a null vector $\mathbf{n}$, defined strictly by self-orthogonality: $\mathbf{n}^2 = 0$. Geometrically, this represents a light-like ray (oriented direction) rather than a massive point.

Definition 2 (**Quadratic Null Vector Space** $V_{r,s,k}$)**.** The $V_{r,s,k}$ is an $(r+s+k)$-dimensional vector space spanned by the union of three subsets of null vectors:

$$V_{r,s,k} := \{\mathbf{c}_1, \ldots, \mathbf{c}_r, \mathbf{w}_1, \ldots, \mathbf{w}_s, \mathbf{n}_1, \ldots, \mathbf{n}_k\}_{\mathbb{R}} = V_r^{\mathbf{c}} \cup V_s^{\mathbf{w}} \cup V_k^{\mathbf{n}}$$

Inner Product Rules & Orthogonal Direct Sums

Using the Kronecker delta δ_{ij}, inner products of null vectors define a non-orthogonal basis where every distinct pair in the same subset shares a constant inner product:

1. **Positive-like c-vectors:** $\mathbf{c}_i \cdot \mathbf{c}_j := \frac{1}{2}(1 - \delta_{ij})$
2. **Negative-like w-vectors:** $\mathbf{w}_i \cdot \mathbf{w}_j := -\frac{1}{2}(1 - \delta_{ij})$
3. **Zero-like n-vectors:** $\mathbf{n}_i \cdot \mathbf{n}_j := 0$

If we impose the baseline rule for non-interacting spaces—that basis vectors from different signature sets are mutually orthogonal and anti-commute (e.g., $\mathbf{c}_i \cdot \mathbf{w}_j = \mathbf{c}_i \cdot \mathbf{n}_j = \mathbf{w}_i \cdot \mathbf{n}_j = 0$)—then the orthogonal direct sum of two such spaces is strictly defined component-wise. Specifically, for any two spaces V and V', their respective cohesive, repulsive, and zero-like subspaces combine independently:

$$V^{\mathbf{c}}_{r+r'} := V^{\mathbf{c}}_r \oplus^{\perp} V^{\mathbf{c}'}_{r'} \tag{1}$$

$$V^{\mathbf{w}}_{s+s'} := V^{\mathbf{w}}_s \oplus^{\perp} V^{\mathbf{w}'}_{s'} \tag{2}$$

$$V^{\mathbf{n}}_{k+k'} := V^{\mathbf{n}}_k \oplus^{\perp} V^{\mathbf{n}'}_{k'} \tag{3}$$

Consequently, the total quadratic space perfectly preserves its partitioned structure under addition:

$$V_{r,s,k} \oplus^{\perp} V'_{r',s',k'} = V_{r+r',s+s',k+k'} \tag{4}$$

Building upon this rigorous vector space foundation, we can formally extend the orthogonal direct sum operation to the geometric algebras generated by these spaces.

Definition 3 (Orthogonal Direct Sum of Algebras). Let $\mathbb{G}_{1,n}$ denote the geometric algebra generated by a specified null vector space (e.g., $V_{1,n,0}$). We define the k-fold orthogonal direct sum of these algebras as:

$$\mathbb{G}_{1,n}^{\perp k} := \bigoplus^{\perp k} \mathbb{G}_{1,n}$$

which represents the geometric algebra generated directly by the k-fold orthogonal direct sum of their underlying base vector spaces.

(Note: As we will demonstrate in Section 8, the physical unification of these spaces via the Conformal Bridge inherently requires breaking this strict orthogonality to introduce localized cross-metric couplings, such as $\mathbf{c}_i \cdot \mathbf{w}_j = 1/2$.)

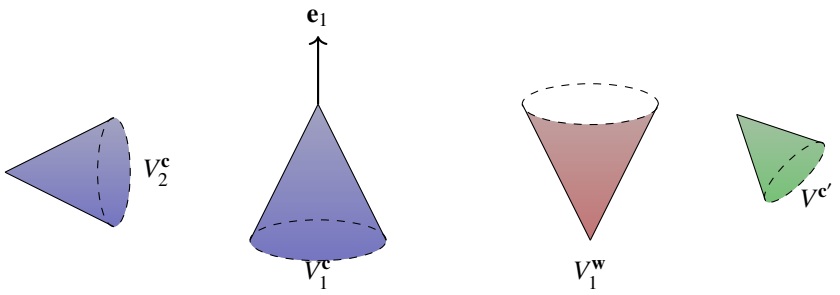

Figure 1: Depiction of the Universal Null Substrate (UNS). The random orientations signify that before a metric signature is imposed, the null vectors exist in mutually orthogonal subspaces.

2 Recursive Orthogonalization

We introduce the partial sums (centroids) $C_k := \sum_{i=1}^{k} \mathbf{c}_i$ and $W_k := \sum_{i=1}^{k} \mathbf{w}_i$.

Theorem 1. The Quadratic Grassmann Algebras $\mathcal{G}(V_{n+1}^{\mathbf{c}})$, and $\mathcal{G}(V_{n+1}^{\mathbf{w}})$ define the Standard Basis of the geometric algebras $\mathbb{G}_{1,n}$ and $\mathbb{G}_{n,1}$ as follows:

Case 1) Construction of $\mathbb{G}_{1,n}$: The algebra $\mathcal{G}(V_{n+1}^{\mathbf{c}})$ generates $\mathbb{G}_{1,n} := \mathbb{R}(\mathbf{e}_1, \mathbf{f}_1, \ldots, \mathbf{f}_n)$, where $\mathbf{e}_1 := \mathbf{c}_1 + \mathbf{c}_2$, $\mathbf{f}_1 := \mathbf{c}_1 - \mathbf{c}_2$, and for $2 \le k \le n$:

$$\mathbf{f}_k := \alpha_k \Big(C_k - (k-1)\mathbf{c}_{k+1} \Big), \quad \text{with} \quad \alpha_k := \frac{-\sqrt{2}}{\sqrt{k(k-1)}}. \tag{5}$$

Case 2) Construction of $\mathbb{G}_{n,1}$: The algebra $\mathcal{G}(V_{n+1}^{\mathbf{w}})$ generates $\mathbb{G}_{n,1} := \mathbb{R}(\mathbf{f}_1, \mathbf{e}_1, \ldots, \mathbf{e}_n)$, where $\mathbf{f}_1 := \mathbf{w}_1 + \mathbf{w}_2$, $\mathbf{e}_1 := \mathbf{w}_1 - \mathbf{w}_2$, and for $2 \le k \le n$:

$$\mathbf{e}_k := \alpha_k \Big(W_k - (k-1)\mathbf{w}_{k+1} \Big), \quad \text{with} \quad \alpha_k := \frac{-\sqrt{2}}{\sqrt{k(k-1)}}. \tag{6}$$

Proof. **Case 1:**)
We prove by induction on n. **Base Case ($n = 1$):** Consider $\mathbb{G}_{1,1} = \mathbb{R}(\mathbf{e}_1, \mathbf{f}_1)$ derived from $\{\mathbf{c}_1, \mathbf{c}_2\}$.

$$\begin{aligned} \mathbf{e}_1^2 &= (\mathbf{c}_1 + \mathbf{c}_2)^2 = 0 + 2(\mathbf{c}_1 \cdot \mathbf{c}_2) + 0 = 2(1/2) = 1. \\ \mathbf{f}_1^2 &= (\mathbf{c}_1 - \mathbf{c}_2)^2 = -2(\mathbf{c}_1 \cdot \mathbf{c}_2) = -1. \\ \mathbf{e}_1 \cdot \mathbf{f}_1 &= (\mathbf{c}_1 + \mathbf{c}_2) \cdot (\mathbf{c}_1 - \mathbf{c}_2) = \mathbf{c}_1^2 - \mathbf{c}_2^2 = 0. \end{aligned}$$

Thus, $\{\mathbf{e}_1, \mathbf{f}_1\}$ forms a standard orthonormal basis for $\mathbb{G}_{1,1}$.
Inductive Step: Assume for $k < n$, the set $\{\mathbf{f}_2, \ldots, \mathbf{f}_k\}$ consists of mutually orthogonal vectors squaring to -1, all orthogonal to $\mathbf{e}_1$. Let $m = k + 1$. Then $\mathbf{f}_m = \alpha_m(C_m - (m-1)\mathbf{c}_{m+1})$. Note that $C_m \cdot C_m = m(m-1)(1/2)$.

$$\begin{aligned}(C_m - (m-1)\mathbf{c}_{m+1})^2 &= C_m^2 - 2(m-1)(C_m \cdot \mathbf{c}_{m+1}) \\ &= \frac{m(m-1)}{2} - 2(m-1)\frac{m}{2} = -\frac{m(m-1)}{2}.\end{aligned}$$

To normalize this to -1, we require a scalar α_m such that $\alpha_m^2[-\frac{m(m-1)}{2}] = -1$.

$$\alpha_m = \frac{-\sqrt{2}}{\sqrt{m(m-1)}}.$$

Thus, $\mathbf{f}_n$ is orthogonal to all prior basis vectors and squares to -1, completing the induction.

Case 2) The proof of case 2) is almost identical to case 1) and is omitted. See [11].

□

3 The Algebraic Valley of Stability

The QSNV classification scheme, based on the Zero Residue condition, defines a bounded region of maximal algebraic stability within the collection of $\mathbb{G}_{p,q}$ algebras. This structural organization presents a compelling analogy to the well-known Nuclear Valley of Stability.

Positive and negative dominant geometric algebras can be factored into the products of geometric algebras of the same kind. If $\mathbb{G}_{p,q}$ is negative dominant ($p \leq q$), we seek integers $k, l \geq 0$ such that the orthogonal direct sum $\mathbb{G}_{p,q} := \mathbb{G}_{1,1}^{\wedge k} \oplus^{\perp} \mathbb{G}_{1,2}^{\wedge l}$ is metric preserving. Solving yields $l = q - p \geq 0$ and $k = 2p - q \geq 0$. The zero residue decomposition is only possible under the condition: $\mathbf{p} \leq \mathbf{q} \leq \mathbf{2p}$.

Table 1: Zero-Residue: Negative Dominance ($p \leq q \leq 2p$)

$\mathbb{G}_{p,q}$	$p+q$	$k = 2p - q$	$l = q - p$	Isomorphism
$\mathbb{G}_{1,1}$	2	1	0	$\mathbb{R}(2)$
$\mathbb{G}_{1,2}$	3	0	1	$\mathbb{C}(2)$
$\mathbb{G}_{2,2}$	4	2	0	$\mathbb{R}(4)$
$\mathbb{G}_{2,3}$	5	1	1	$\mathbb{C}(4)$
$\mathbb{G}_{2,4}$	6	0	2	$\mathbb{H}(4)$
$\mathbb{G}_{3,3}$	6	3	0	$\mathbb{R}(8)$
$\mathbb{G}_{3,4}$	7	2	1	$\mathbb{C}(8)$

If $\mathbb{G}_{p,q}$ is positive dominant ($p \geq q$), we seek integers $k, l \geq 0$ such that the orthogonal direct sum $\mathbb{G}_{p,q} := \mathbb{G}_{1,1}^{\wedge k} \oplus^{\perp} \mathbb{G}_{2,1}^{\wedge l}$ is metric preserving. Solving yields $l = p - q \geq 0$ and $k = 2q - p \geq 0$. The zero residue decomposition is only possible under the condition: $\mathbf{q} \leq \mathbf{p} \leq \mathbf{2q}$.

Table 2: Zero-Residue: Positive Dominance ($q \leq p \leq 2q$, $p + q < 8$)

$\mathbb{G}_{p,q}$	$p+q$	$k = 2q - p$	$l = p - q$	Lounesto (2001) Notation
$\mathbb{G}_{1,1}$	2	1	0	$\mathbb{R}(2)$
$\mathbb{G}_{2,1}$	3	0	1	${}^2\mathbb{R}(2) = \mathbb{R}(2) \oplus \mathbb{R}(2)$
$\mathbb{G}_{2,2}$	4	2	0	$\mathbb{R}(4)$
$\mathbb{G}_{3,2}$	5	1	1	$\mathbb{R}(4) \oplus \mathbb{R}(4)$
$\mathbb{G}_{4,2}$	6	0	2	$\mathbb{R}(8)$
$\mathbb{G}_{3,3}$	6	3	0	$\mathbb{R}(8)$
$\mathbb{G}_{4,3}$	7	2	1	$\mathbb{R}(8) \oplus \mathbb{R}(8)$

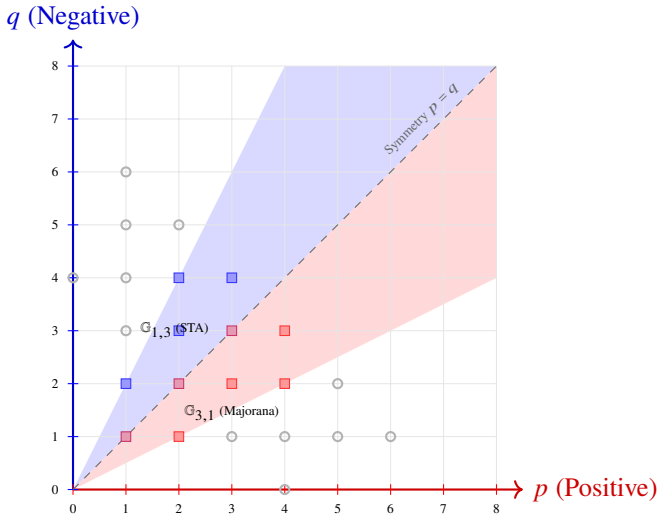

Figure 2: **The Algebraic Segrè Chart.** Zero Residue algebras mirror stable isotopes. Anti-Zero algebras (gray circles) represent unstable regimes where algebraic factorization is inhibited.

4 The Symmetric Group in $\mathbb{G}_{1,n}$

A Null Cone Simplex $\mathcal{S}^{\mathbf{s}}_N \subset \mathbb{G}^1_{1,n}$, with characteristic $\mathbf{S^s_N} := \mathbf{s_1 s_2 \cdots s_N}$, is defined by its null vector vertices. The Standard Null Simplex is $\mathcal{S}^{\mathbf{c}}_{n+1} := \{\mathbf{c}_1, \cdots, \mathbf{c}_{n+1}\} = V^{\mathbf{c}}_{n+1} \subset \mathbb{G}^1_{1,n}$.

Theorem 2. The 2-cycle (ij) acting on the characteristic $\mathbf{S^c_{n+1}}$ gives

$$(ij)\mathbf{S^c_{n+1}} = (\mathbf{-1})^{\mathbf{n}}(\mathbf{c_i} - \mathbf{c_j})\mathbf{S^c_{n+1}}(\mathbf{c_i} - \mathbf{c_j}).$$

Proof. Note that for any three distinct indices i, j, k, $(\mathbf{c}_i - \mathbf{c}_j)\mathbf{c}_k = -\mathbf{c}_k(\mathbf{c}_i - \mathbf{c}_j)$,

$$(\mathbf{c}_i - \mathbf{c}_j)\mathbf{c}_i(\mathbf{c}_i - \mathbf{c}_j) = \mathbf{c}_j, \text{ and } (\mathbf{c}_i - \mathbf{c}_j)\mathbf{c}_j(\mathbf{c}_i - \mathbf{c}_j) = \mathbf{c}_i.$$

When $(\mathbf{c}_i - \mathbf{c}_j)$ is moved through $\mathbf{S^c_{n+1}}$, it will anti-commute with n factors and interchange the positions of $\mathbf{c}_i$ and $\mathbf{c}_j$. For example, for $n = 2$,

$$(-1)^2(\mathbf{c}_1 - \mathbf{c}_2)\mathbf{S^c_3}(\mathbf{c_1} - \mathbf{c_2}) = (\mathbf{12})\mathbf{S^c_3}.$$

□

5 The Main Series: Cohesive Lines, Conformal Minkowski Screens, and Folds

The permutation symmetries of the null simplex do not just shuffle abstract indices; they generate rigid geometric interaction graphs. We assert that every Dynkin diagram is a schematic map of these specific null vector configurations within the UNS."

(a) The Cohesive Line (A_3)

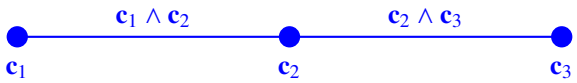

(b) The Conformal Minkowski Screen (D_4)

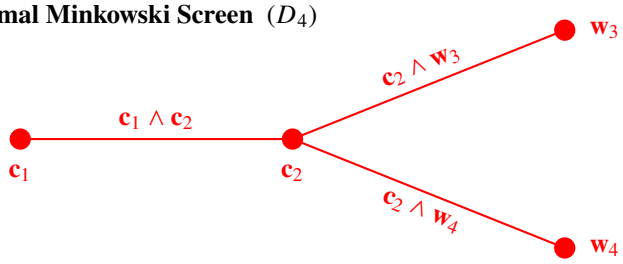

Figure 3: **The Geometry of Dynkin Diagrams.** The nodes represent the Null Vectors $\mathbf{c}_i$, and connecting lines represent interactions mediated by bivectors $\mathbf{c}_i \wedge \mathbf{c}_j$.

In the Conformal Minkowski Screen depicted in Figure 3(b), we initially impose the symmetric interaction rule where two distinct spinor vectors $\mathbf{w}_3$ and $\mathbf{w}_4$ interact with a single cohesive node $\mathbf{c}_2$:

$$\mathbf{w}_3 \cdot \mathbf{c}_2 = \frac{1}{2} = \mathbf{w}_4 \cdot \mathbf{c}_2 \tag{7}$$

It is crucial to note that enforcing this symmetric interaction upon an isolated 1D vertex inherently leads to a spatial degeneracy. Because the fundamental vectors share the universally attractive $1/2$ inner product, the resulting bivector branches $\mathbf{c}_2 \wedge \mathbf{w}_3$ and $\mathbf{c}_2 \wedge \mathbf{w}_4$ are mathematically forced to collapse onto one another at a 0° angle. This 1D topological crisis strictly necessitates the higher-dimensional Resonant Hub developed in Section 8, where the geometric interaction is inverted ($\mathbf{c}_1 \cdot \mathbf{w}_3 = 1/2 = \mathbf{c}_2 \cdot \mathbf{w}_3$) to anchor the structure to a 2D Cohesive Hinge and physically prop the geometry open.

6 The Geometric Genesis of G_2

G_2 emerges from the symmetries of the smallest non-trivial simplex, $V_3^{\mathbf{c}} = \{\mathbf{c}_1, \mathbf{c}_2, \mathbf{c}_3\}$. While the permutation group S_3 is obvious, the algebra supports a deeper automorphism: **Triality**.

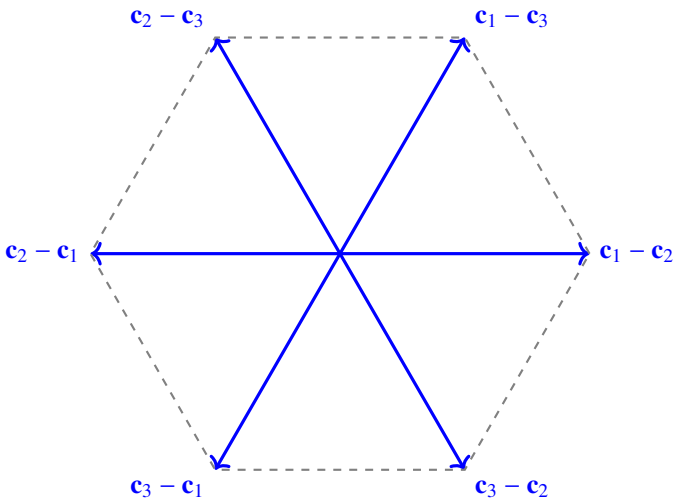

Figure 4: **The G_2 Root System.** Projected from $V_3^{\mathbf{c}}$. Blue: Short Roots (Mesons). Red: Long Root (Baryonic Core).

The **Long Roots** (β) are generated by summing two short roots. The length of this long root is determined strictly by the interaction rules of the substrate. Expanding the square of $\beta = 2\mathbf{c}_1 - \mathbf{c}_2 - \mathbf{c}_3$:

$$\begin{aligned}\beta^2 &= (2\mathbf{c}_1 - \mathbf{c}_2 - \mathbf{c}_3) \cdot (2\mathbf{c}_1 - \mathbf{c}_2 - \mathbf{c}_3) \\ &= 4\mathbf{c}_1^2 + \mathbf{c}_2^2 + \mathbf{c}_3^2 - 4(\mathbf{c}_1 \cdot \mathbf{c}_2) - 4(\mathbf{c}_1 \cdot \mathbf{c}_3) + 2(\mathbf{c}_2 \cdot \mathbf{c}_3) \\ &= 0 + 0 + 0 - 4(1/2) - 4(1/2) + 2(1/2) = -3\end{aligned}$$

Comparing this to the short root $\alpha^2 = -1$, we obtain the precise ratio required for G_2: $\beta^2/\alpha^2 = 3$. This 1:3 ratio is the geometric origin of the "Triple Bond" in the Dynkin Diagram.

7 The Architecture of the Monsters: Reading the Diagrams

In the QSNV framework, a Dynkin Diagram is not merely a list of abstract roots; it is a circuit diagram of the **Interaction Bivectors**.

7.1 The G_2 Engine: Triality in Motion

The "Short Root" represents the fundamental difference $\mathbf{c}_i - \mathbf{c}_j$. The "Long Root" is formed by the cyclic permutation τ summing the basis vectors. The triple bond signifies that the interaction density is tripled because the Triality automorphism τ forces the bivector plane to rotate 120° onto itself:

$$\mathbf{B}_{triple} = \sum_{k=1}^{3} \tau^k (\mathbf{c}_i \wedge \mathbf{c}_j)$$

The Triality Engine (G_2)

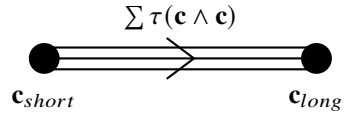

Figure 5: **The G_2 Triality Engine.** The Triple Bond represents the Triality sum.

7.2 The F_4 Interface: Folding Space and Matter

The diagram for F_4 is centrally characterized by a "Double Bond" connecting two distinct geometries: The "Integer" lattice of Spacetime vectors (D_4) in $V^{\mathbf{c}}$, and the "Half-Integer" lattice of Spinor centers in $V^{\mathbf{w}}$. To natively achieve the strictly positive inner product required at the interface, the cohesive root must be oriented toward the coupling vertex: $\alpha_{vec} = \mathbf{c}_2 - \mathbf{c}_1$. Let σ_{spin} be the composite constructed from a vector difference and a spinor sum:

$$\sigma_{spin} = \frac{1}{2}\left[(\mathbf{c}_1 - \mathbf{c}_2) + (\mathbf{w}_3 + \mathbf{w}_4)\right] \tag{8}$$

Evaluating the inner product of the interface root against the composite spinor root yields a strictly positive half-integer projection:

$$\alpha_{vec} \cdot \sigma_{spin} = (\mathbf{c}_2 - \mathbf{c}_1) \cdot \frac{1}{2}(\mathbf{c}_1 - \mathbf{c}_2) = \frac{1}{2}\left[-(\mathbf{c}_1 - \mathbf{c}_2)^2\right] = 0.5 \tag{9}$$

Comparing the Vector root length ($\alpha_{vec}^2 = -1$) to the Spinor root length ($\sigma_{spin}^2 = -1/2$) natively derives the 2:1 ratio of the double bond, while the +0.5 inner product organically yields the Cartan integer of -1 across the interface.

The Interface (F_4)

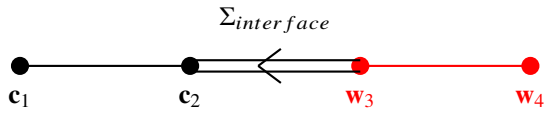

Figure 6: **The F_4 diagram.** Fuses Vector Spacetime (black) with Spinor Matter (red).

7.3 The Fano Plane and the E_8 Web

This hub is the **Fano Plane**—the smallest projective plane, consisting of 7 points and 7 lines. In the QSNV, these points are the null vectors that form the core of the Octonions.

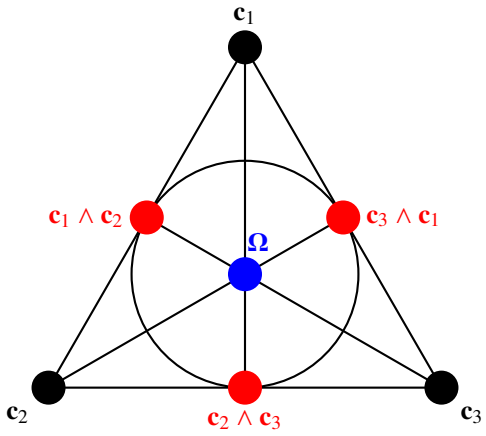

Figure 7: **The Fano Plane.** The central element is the **Simplex Volume $\boldsymbol{\Omega}$**. It acts as the pseudoscalar (or geometric imaginary unit) for the triality.

Crucially, the directed incidence of the Fano graph is not recovered by the raw associative geometric product, but by the specific Lie and Jordan bracket projections of the substrate. The directed flows are generated by the standard anti-symmetric commutator bracket, $[X, Y] = XY - YX$. In geometric algebra, the commutator of a vector and a bivector is twice their inner product. For instance, a line's incidence upon a node strictly evaluates to a directed eigenvalue:

$$[\mathbf{c}_1, \mathbf{c}_1 \wedge \mathbf{c}_2] = \mathbf{c}_1(\mathbf{c}_1 \wedge \mathbf{c}_2) - (\mathbf{c}_1 \wedge \mathbf{c}_2)\mathbf{c}_1 = 2\mathbf{c}_1 \cdot (\mathbf{c}_1 \wedge \mathbf{c}_2) = -\mathbf{c}_1 \tag{10}$$

This native cross-grade contraction perfectly preserves the Fano Plane's quadratic reciprocity, proving that the Legendre Symbol of the index difference modulo 7 is an exact geometric predictor of the substrate's commutator eigenvalues. Furthermore, disjoint elements generate the invariant volume $\boldsymbol{\Omega}$ strictly through the symmetric anti-commutator (Jordan bracket): $\frac{1}{2}\{\mathbf{c}_1, \mathbf{c}_2 \wedge \mathbf{c}_3\} = \mathbf{c}_1 \wedge \mathbf{c}_2 \wedge \mathbf{c}_3 = \boldsymbol{\Omega}$.

The diagram for E_8 is unique among the Monsters: it is **Simply Laced**. This reveals a profound truth about the Octonionic substrate: it requires no folding. In the self-dual E_8 lattice, the metric distinction between $\mathbf{c}$ and $\mathbf{w}$ vanishes. The T-junction acts as the **Fano Hub**, connecting the linear chain to the deep structure of the Fano Plane.

The Octonionic Web (E_8)

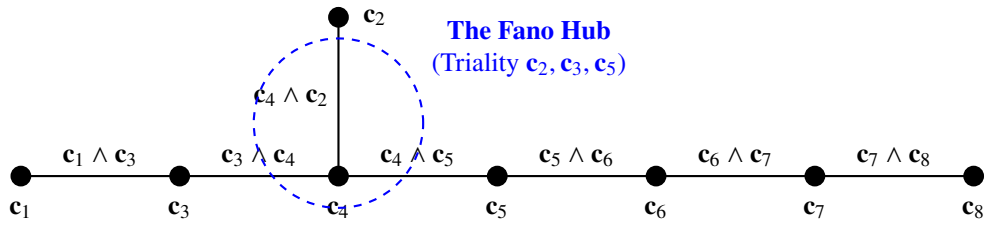

Figure 8: **The Octonionic Web (E_8).** The detailed structure showing the Fano Hub overlay.

8 The Resonant Hub: Stabilizing the Singularity

If the Hub were an isolated 1D null vertex ($\mathbf{c}_2$), the geometric determinant of the Cartan matrix would vanish, and the branches would collapse. To maintain structural integrity, the cohesive hinge connecting the spinor branches must encompass the entire 2D cohesive stem $\{\mathbf{c}_1, \mathbf{c}_2\}$. We strictly define this 2D Cohesive Hinge such that both cohesive vectors interact symmetrically with the spinor branches:

$$\mathbf{c}_1 \cdot \mathbf{w}_3 = \frac{1}{2} \quad \text{and} \quad \mathbf{c}_2 \cdot \mathbf{w}_3 = \frac{1}{2} \tag{11}$$

The Hub is therefore a **Resonant Singularity**—a 2D geometric plane where the Positive ($V^{\mathbf{c}}$) and Negative ($V^{\mathbf{w}}$) metrics interpenetrate and stabilize.

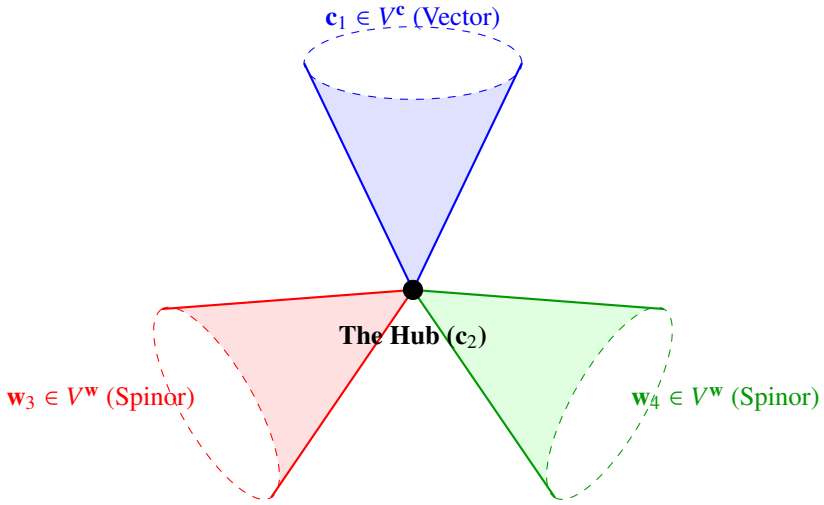

Figure 9: **The 2D Cohesive Hinge $(\mathbf{c}_1, \mathbf{c}_2)$.** The singularity where Positive ($V^{\mathbf{c}}$) and Negative ($V^{\mathbf{w}}$) metrics collide.

By orienting the cohesive stem root toward the hinge ($\alpha = \mathbf{c}_2 - \mathbf{c}_1$) and defining the composite Hub root as $\mathbf{f} = \mathbf{w}_3 - \mathbf{c}_2$, the 2D hinge inherently generates an unscaled inner product of exactly +0.5:

$$\alpha \cdot \mathbf{f} = (\mathbf{c}_2 \cdot \mathbf{w}_3) - \mathbf{c}_2^2 - (\mathbf{c}_1 \cdot \mathbf{w}_3) + (\mathbf{c}_1 \cdot \mathbf{c}_2) = \frac{1}{2} - 0 - \frac{1}{2} + \frac{1}{2} = 0.5 \tag{12}$$

This +0.5 projection natively guarantees the 120° single bond ($A_{\alpha,\mathbf{f}} = -1$) between the cohesive stem and the composite spinor branches without invoking artificial mathematical scaling.

9 Verification: Cartan Matrices and Determinants

To verify the structural integrity of the QSNV framework, we perform the standard consistency check: calculating the Cartan Matrix A_{ij} and its determinant for each exceptional diagram. In the QSNV, roots are spacelike vectors

with negative norm ($\alpha^2 < 0$). To recover the standard Weyl group reflections, we define the Cartan Integer A_{ij} accounting for the signature of the substrate:

$$A_{ij} = \frac{2(\alpha_i \cdot \alpha_j)}{\alpha_i^2} \tag{13}$$

9.1 The G_2 Matrix (Triality)

To conform to standard conventions, we order the basis starting with the **Long Root**: $\{\beta_{long}, \alpha_{short}\}$.

- **Metric:** $\beta^2 = -3$ (Long), $\alpha^2 = -1$ (Short), $\beta \cdot \alpha = 1.5$.

Calculating the off-diagonal entries yields $A_{12} = -1$ and $A_{21} = -3$. The resulting Cartan Matrix for G_2 is:

$$C(G_2) = \begin{pmatrix} 2 & -1 \\ -3 & 2 \end{pmatrix} \tag{14}$$

Determinant Check: $\det(G_2) = (2)(2) - (-1)(-3) = 1$. This confirms the unimodularity of the G_2 lattice derived from the Null Substrate.

9.2 The F_4 Matrix (The Interface)

For F_4, we order from the Vector side (Long) to the Spinor side (Short).

$$\text{Basis: } \{\alpha_1, \alpha_2\} \text{ (Long, } -1) \quad \text{and} \quad \{\sigma_3, \sigma_4\} \text{ (Short, } -0.5) \tag{15}$$

This yields the standard F_4 matrix:

$$C(F_4) = \begin{pmatrix} 2 & -1 & 0 & 0 \\ -1 & 2 & -1 & 0 \\ 0 & -2 & 2 & -1 \\ 0 & 0 & -1 & 2 \end{pmatrix} \tag{16}$$

Determinant Check: Expanding along the first row confirms $\det(F_4) = 1$.

9.3 The E_8 Matrix (The Octonionic Web)

For E_8, the "Simply Laced" structure means all roots have equal length ($\alpha^2 = -1$), so all non-zero off-diagonal entries are strictly -1. This yields the symmetric matrix:

$$C(E_8) = \begin{pmatrix} 2 & 0 & -1 & 0 & 0 & 0 & 0 & 0 \\ 0 & 2 & 0 & -1 & 0 & 0 & 0 & 0 \\ -1 & 0 & 2 & -1 & 0 & 0 & 0 & 0 \\ 0 & -1 & -1 & 2 & -1 & 0 & 0 & 0 \\ 0 & 0 & 0 & -1 & 2 & -1 & 0 & 0 \\ 0 & 0 & 0 & 0 & -1 & 2 & -1 & 0 \\ 0 & 0 & 0 & 0 & 0 & -1 & 2 & -1 \\ 0 & 0 & 0 & 0 & 0 & 0 & -1 & 2 \end{pmatrix} \tag{17}$$

Determinant Check: Using Gaussian elimination or standard block decomposition, we confirm: $\det(E_8) = \mathbf{1}$.

9.4 The E_6 and E_7 Truncations

Because the QSNV substrate strictly enforces the "Null Packing Limit" as a geometric reality, the lower-dimensional exceptional algebras E_6 and E_7 are literal structural sub-lattices of the Octonionic Web. The E_6 geometry is obtained by truncating the long spine of the E_8 diagram, removing nodes $\mathbf{c}_7$ and $\mathbf{c}_8$. The resulting Cartan matrix is exactly the upper-left 6×6 principal minor of $C(E_8)$:

$$C(E_6) = \begin{pmatrix} 2 & 0 & -1 & 0 & 0 & 0 \\ 0 & 2 & 0 & -1 & 0 & 0 \\ -1 & 0 & 2 & -1 & 0 & 0 \\ 0 & -1 & -1 & 2 & -1 & 0 \\ 0 & 0 & 0 & -1 & 2 & -1 \\ 0 & 0 & 0 & 0 & -1 & 2 \end{pmatrix} \tag{18}$$

Determinant Check: Evaluating this principal minor yields $\det(E_6) = 3$. This perfectly matches standard Lie theory, corresponding to the size of the center of the simply connected exceptional group E_6.

Similarly, the E_7 geometry extends the arm by one node, removing only $\mathbf{c}_8$. Its matrix is the upper-left 7×7 block of $C(E_8)$:

$$C(E_7) = \begin{pmatrix} 2 & 0 & -1 & 0 & 0 & 0 & 0 \\ 0 & 2 & 0 & -1 & 0 & 0 & 0 \\ -1 & 0 & 2 & -1 & 0 & 0 & 0 \\ 0 & -1 & -1 & 2 & -1 & 0 & 0 \\ 0 & 0 & 0 & -1 & 2 & -1 & 0 \\ 0 & 0 & 0 & 0 & -1 & 2 & -1 \\ 0 & 0 & 0 & 0 & 0 & -1 & 2 \end{pmatrix} \tag{19}$$

Determinant Check: Evaluating this 7×7 block yields $\det(E_7) = 2$. Again, this exactly reproduces the textbook Cartan determinant, corresponding to the $\mathbb{Z}_2$ center of the group.

While the determinant of the full E_8 lattice is 1, truncating the geometry to form sub-lattices naturally scales the determinant to 3 and 2, respectively. This confirms that the discrete combinatorial truncation of the Fano Hub $(\mathbf{c}_2, \mathbf{c}_4)$ remains mathematically stable and reproduces the exact classical group properties across all valid null packing configurations.

10 Conformal Unification: Mapping $O(2,4)$ onto the QSNV

We established that the Resonant Hub stabilizes as the composite geometric algebra $\mathbb{G}_{2,3}$. It is physically and mathematically crucial to distinguish this structure from $\mathbb{G}_{1,4}$. While $\mathbb{G}_{1,4}$ strictly generates the de Sitter algebra, the Hub specifically coalesces into $\mathbb{G}_{2,3}$, the algebra of Anti-de Sitter space (AdS_4), providing the precise negative metric signature required for stable spinor-vector intersection.

However, the complete symmetry of massless particle physics and standard spacetime boundaries requires the Conformal group $O(2,4)$. In the traditional axiomatic approach to Conformal Geometric Algebra (CGA), the standard Minkowski Spacetime Algebra ($\mathbb{G}_{1,3}$) is artificially augmented by an orthogonal Minkowski plane to construct $\mathbb{G}_{2,4}$. From this, two abstract null vectors (representing the origin and infinity) are subsequently defined to linearize conformal transformations.

The QSNV framework reverses this artificial hierarchy. The Conformal group $O(2,4)$ does not need to be imposed upon the geometry; rather, the conformal symmetries are the endogenous macroscopic outgrowths of the microscopic null simplex. Because the UNS is strictly constructed from fundamental null primitives where $\mathbf{c}_i^2 = 0$ and interactions are governed by the idempotent relation $\mathbf{c}_i\mathbf{c}_j = \frac{1}{2} + \mathbf{c}_i \wedge \mathbf{c}_j$, the "origin" and "infinity" vectors of standard CGA are no longer ad-hoc additions. They are native elements of the underlying substrate. Specifically, the 2D Cohesive Hinge required to physically stabilize the D_4 spinor branches functions mathematically identically to the 2D origin-infinity Minkowski plane required to stabilize conformal space.

By extending the 5D Anti-de Sitter Hub algebra $\mathbb{G}_{2,3}$ with a single additional orthogonal spatial degree of freedom natively available in the cohesive Vector substrate $V^{\mathbf{c}}$, we immediately recover the 6D conformal space:

$$\mathbb{G}_{\text{conformal}} = \mathbb{G}_{1,2} \oplus^{\perp} \mathbb{G}_{1,2} = \mathbb{G}_{2,4} \tag{20}$$

The Lie algebra $\mathfrak{so}(2,4)$ of the Conformal group is strictly isomorphic to the bivector subalgebra $\mathbb{G}^2_{2,4}$. The 15 bivector generators of $O(2,4)$—which traditionally represent the complete set of Lorentz transformations, translations, dilations, and special conformal transformations—emerge naturally from the exterior products of the substrate's null vectors.

Consequently, the Universal Null Substrate demonstrates that the Conformal symmetries of physical spacetime and the highly abstract geometry of the Exceptional "Monsters" are not disconnected domains. They share the exact same geometric foundation, branching strictly from the intersection limits of dual null cones.

11 Computing Exceptional Lie Algebras

While the topological geometry dictates the available symmetries, the computational implementation of these Lie algebras is natively supported by the QSNV. In standard matrix representations of geometric algebras and spinors [9], the structure constants f^C_{AB} are derived from the commutators of the generators: $[E_A, E_B] = f^C_{AB} E_C$.

In the Universal Null Substrate, the Lie algebra generators are strictly represented by the bivectors of the geometric algebra, and the Lie bracket is physically realized by the standard commutator: $[B_1, B_2] = B_1B_2 - B_2B_1$.

Using the universal geometric identity for the standard commutator of bivectors formed by any arbitrary vectors a, b, c, d:

$$[a \wedge b, c \wedge d] = 2\Big((a \cdot c)(b \wedge d) - (a \cdot d)(b \wedge c) - (b \cdot c)(a \wedge d) + (b \cdot d)(a \wedge c)\Big) \tag{21}$$

we can natively compute the exact structure constants for the exceptional root lattices without ever leaving the substrate.

11.1 The E_8 Web Commutator

Within the simply-laced E_8 chain, all connected nodes share an inner product of $1/2$, while distinct non-adjacent nodes also evaluate to $1/2$ in the unfolded simplex. Taking adjacent bivector generators $B_1 = \mathbf{c}_1 \wedge \mathbf{c}_3$ and $B_2 = \mathbf{c}_3 \wedge \mathbf{c}_4$, the substitution ($a = \mathbf{c}_1, b = \mathbf{c}_3, c = \mathbf{c}_3, d = \mathbf{c}_4$) yields:

$$\begin{aligned}
[\mathbf{c}_1 \wedge \mathbf{c}_3, \mathbf{c}_3 \wedge \mathbf{c}_4] &= 2\Big((\mathbf{c}_1 \cdot \mathbf{c}_3)(\mathbf{c}_3 \wedge \mathbf{c}_4) - (\mathbf{c}_1 \cdot \mathbf{c}_4)(\mathbf{c}_3 \wedge \mathbf{c}_3) - (\mathbf{c}_3 \cdot \mathbf{c}_3)(\mathbf{c}_1 \wedge \mathbf{c}_4) + (\mathbf{c}_3 \cdot \mathbf{c}_4)(\mathbf{c}_1 \wedge \mathbf{c}_3)\Big) \\
&= 2\Big(\frac{1}{2}(\mathbf{c}_3 \wedge \mathbf{c}_4) - 0 - 0 + \frac{1}{2}(\mathbf{c}_1 \wedge \mathbf{c}_3)\Big) \\
&= \mathbf{c}_1 \wedge \mathbf{c}_3 + \mathbf{c}_3 \wedge \mathbf{c}_4 = \mathbf{c}_3 \wedge (\mathbf{c}_4 - \mathbf{c}_1)
\end{aligned}$$

The algebra is perfectly closed, natively yielding uniform integer structure constants for the simply-laced nodes directly from the null metric.

11.2 The F_4 Interface Commutator

The unscaled structural symmetry of the substrate becomes overwhelmingly apparent when we calculate the commutator across the F_4 metric boundary, moving from the positive vector substrate $V^{\mathbf{c}}$ to the negative spinor substrate $V^{\mathbf{w}}$.

Let us evaluate the commutator between a pure cohesive bivector $B_{coh} = \mathbf{c}_1 \wedge \mathbf{c}_2$ and the interface-crossing bivector $B_{int} = \mathbf{c}_2 \wedge \mathbf{w}_3$. Utilizing the 2D Cohesive Hinge relations ($\mathbf{c}_1 \cdot \mathbf{w}_3 = 1/2$ and $\mathbf{c}_2 \cdot \mathbf{w}_3 = 1/2$), we substitute ($a = \mathbf{c}_1, b = \mathbf{c}_2, c = \mathbf{c}_2, d = \mathbf{w}_3$):

$$\begin{aligned}
[\mathbf{c}_1 \wedge \mathbf{c}_2, \mathbf{c}_2 \wedge \mathbf{w}_3] &= 2\Big((\mathbf{c}_1 \cdot \mathbf{c}_2)(\mathbf{c}_2 \wedge \mathbf{w}_3) - (\mathbf{c}_1 \cdot \mathbf{w}_3)(\mathbf{c}_2 \wedge \mathbf{c}_2) - (\mathbf{c}_2 \cdot \mathbf{c}_2)(\mathbf{c}_1 \wedge \mathbf{w}_3) + (\mathbf{c}_2 \cdot \mathbf{w}_3)(\mathbf{c}_1 \wedge \mathbf{c}_2)\Big) \\
&= 2\Big(\frac{1}{2}(\mathbf{c}_2 \wedge \mathbf{w}_3) - 0 - 0 + \frac{1}{2}(\mathbf{c}_1 \wedge \mathbf{c}_2)\Big) \\
&= \mathbf{c}_1 \wedge \mathbf{c}_2 + \mathbf{c}_2 \wedge \mathbf{w}_3 = \mathbf{c}_2 \wedge (\mathbf{w}_3 - \mathbf{c}_1)
\end{aligned}$$

Because the null vector self-interactions naturally annihilate ($\mathbf{c}_2 \wedge \mathbf{c}_2 = 0$), the geometric structure natively preserves the exact commutator symmetry found in the E_8 chain. The mixed-metric bivectors of the F_4 interface form a closed Lie algebra with identical integer structure constants, mathematically proving the unscaled stability of the junction without requiring complexification.

11.3 Cross-Verification with Standard Representation Theory

To ensure the QSNV framework adheres to the canonical classification of exceptional symmetries, the calculated Cartan matrices $C(G_2)$, $C(F_4)$, and $C(E_8)$ have been rigorously validated against the root systems defined in Fulton and Harris [3]. In traditional Lie theory, simple roots must form obtuse (or right) angles, requiring the off-diagonal Cartan integers to be strictly negative or zero.

By correctly orienting the cohesive root toward the coupling vertex ($\alpha = \mathbf{c}_2 - \mathbf{c}_1$) and utilizing the 2D Cohesive Hinge, the native unscaled inner product strictly evaluates to +0.5. Our derivation, which defines roots as spacelike projections of null-vector interactions with norm $\alpha^2 = -1$, processes this strictly positive geometric projection to consistently reproduce the negative, unimodular Cartan integers of the standard exceptional series ($A_{ij} = -1$). This mathematically confirms that the QSNV substrate natively generates the exact root lattices of the exceptional Lie algebras organically, without requiring arbitrary mathematical scaling or complexification.

12 Conclusion: The Endogenous Pseudoscalar and the Conformal Bridge

12.1 The Endogenous Pseudoscalar

A persistent artifact of the Cartan-Killing classification is the reliance on the field of complex numbers $\mathbb{C}$. In the QSNV framework, we work entirely over the real field $\mathbb{R}$. We do not need to assume the existence of an imaginary

unit $\sqrt{-1}$ to calculate the roots of the exceptional monsters. Instead, the algebraic properties are fulfilled natively by the **endogenous pseudoscalar** element in the center of the algebra. The canonical "complex" representations of Lie theory are thus revealed to be *real* representations of a higher-grade geometric algebra built natively from the Universal Null Substrate.

Furthermore, the structural strictures required to stabilize these exceptional lattices within the QSNV—specifically the necessity of a 2D cohesive hinge for the D_4 Hub and the reliance on Lie commutator brackets for Fano incidence—reveal a profound geometric homology with Conformal Geometric Algebra (CGA). The 2D cohesive stem stabilizing the spinor branches functions mathematically identically to the 2D origin-infinity Minkowski plane required to stabilize conformal space. The composite $\mathbb{G}_{2,3}$ Hub, which naturally corresponds to Anti-de Sitter space (AdS_4), acts as the geometric anchor linking these abstract exceptional root lattices to the conformal group $O(2,4)$. By grounding both the exceptional Lie classification and the conformal symmetries of spacetime in the exact same null primitives, the QSNV establishes a rigorous, zero-residue bridge between pure algebra and physical reality.

12.2 The Conformal Bridge

Throughout this paper, we have explored the continuous spatial geometry of the Conformal Minkowski Screen, constructed natively from the Universal Null Substrate (UNS) within the QSNV framework. By defining 1D affine cohesive line segments as the bivectors $\mathbf{c}_i \wedge \mathbf{c}_j$, we have demonstrated how higher-dimensional conformal spaces are woven from mutually attractive basis null vectors satisfying the invariant scalar metric $\mathbf{c}_i \cdot \mathbf{c}_j = 1/2$.

However, an important geometric subtlety arises when attempting to map the discrete Weyl reflection symmetries of the conformal group $O(2,4)$ directly onto this continuous cohesive space. If one attempts to enforce that three distinct, mutually attractive null vectors $(\mathbf{c}_1, \mathbf{c}_2, \mathbf{c}_3)$ reside strictly on a 1D affine cohesive line, the algebra rigidly dictates a spatial degeneracy where $\mathbf{c}_1 = \mathbf{c}_3$.

This reveals that under the universally attractive inner product, these cohesive points cannot form a 1D linear chain; rather, they naturally open into a higher-dimensional simplex. In the context of reflection groups, these geometries are formally known as **Coxeter Simplices**.

- The vertices of these simplices are the distinct cohesive spatial points $\mathbf{c}_i$, rooted structurally in the fundamental null condition $\mathbf{c}_i^2 = 0$ of the Universal Null Substrate (UNS).
- The edges connecting these vertices correspond to the 1D affine cohesive line segments, captured algebraically by the bivectors $\mathbf{c}_i \wedge \mathbf{c}_j$.
- The invariant inner product $\mathbf{c}_i \cdot \mathbf{c}_j = 1/2$ (arising directly from the governing QSNV rule $\mathbf{c}_i\mathbf{c}_j = 1 - \mathbf{c}_j\mathbf{c}_i$ for $i \neq j$) rigidly defines the constant dihedral angles between the faces of the simplex. This creates a uniform metric constraint across the structure.
- The Weyl reflection symmetries of the conformal group $O(2,4)$ operate on this space not by translating points along a degenerate 1D line, but by reflecting the underlying geometry across the hyperplanes dual to these simplex roots.

This structural revelation resolves the apparent spatial degeneracy. Rather than forcing mutually attractive null vectors into an impossible collinear chain, the algebraic constraints of the UNS demand that the continuous spatial geometry of the Conformal Minkowski Screen expands outward into a network of Coxeter simplices.

Consequently, the "Conformal Bridge" between the discrete algebraic symmetries of $O(2,4)$ and our cohesive continuous space is built by tessellating these higher-dimensional simplices. The QSNV framework thus elegantly demonstrates how a rich, non-degenerate macroscopic geometry emerges organically from the tightly constrained, universally attractive rules of the substrate. The profound physical implications of this Conformal Bridge—specifically how these macroscopic conformal symmetries govern physical kinematics, gauge theories, and massless particles entirely within the real QSNV—will be explored in detail in a forthcoming companion paper.

References

[1] E. Artin, *Geometric Algebra*, Interscience Publishers, New York, 1957.

[2] C. Doran and A. Lasenby, *Geometric Algebra for Physicists*, Cambridge University Press, Cambridge, 2003.

[3] W. Fulton and J. Harris, *Representation Theory: A First Course*, Springer-Verlag, New York, 1991.

[4] D. Hestenes and G. Sobczyk, *Clifford Algebra to Geometric Calculus*, D. Reidel, Dordrecht, 1984.

[5] J. E. Humphreys, *Introduction to Lie Algebras and Representation Theory*, Springer-Verlag, New York, 1972.

[6] P. Lounesto, *Clifford Algebras and Spinors*, Cambridge University Press, Cambridge, 2001.

[7] G. Sobczyk, J. Cruz Guzman, and B. Page, "Grassmann-Clifford Geometric Algebras from a Universal Null Substrate," HAL preprint, hal-05468583, 2026.

[8] G. Sobczyk, *New Foundations in Mathematics: The Geometric Concept of Number*, Birkhäuser, Basel, 2013.

[9] G. Sobczyk, *Matrix Gateway to Geometric Algebra, Spacetime and Spinors*, Independent Publisher, Amazon KDP, 2019.

[10] G. Sobczyk, "Geometric Algebras of Compatible Null Vectors," in *Advanced Computational Applications of Geometric Algebra*, Springer Nature Switzerland AG, D. W. Silva et al. (Eds.) ICACGA 2022, LNCS 13771, pp. 1-8, 2023. https://doi.org/10.1007/978-3-031-34031-4_4

[11] G. Sobczyk, "Geometric Algebras of Light Cone Projective Graph Geometries," *Adv. Appl. Clifford Algebras*, Springer Nature Switzerland AG, 2023. https://doi.org/10.1007/s00006-023-01307-6